



LAWRENCE
LIVERMORE
NATIONAL
LABORATORY

Magnetic Field Line Tracing Calculations for Conceptual PFC Design in the National Compact Stellarator Experiment

R. Maingi, T. Kaiser, D. N. Hill, J. F. Lyon, D.
Monticello, M. C. Zarnstorff

June 15, 2006

2006 EPS Conference
Rome, Italy
June 19, 2006 through June 23, 2006

Disclaimer

This document was prepared as an account of work sponsored by an agency of the United States Government. Neither the United States Government nor the University of California nor any of their employees, makes any warranty, express or implied, or assumes any legal liability or responsibility for the accuracy, completeness, or usefulness of any information, apparatus, product, or process disclosed, or represents that its use would not infringe privately owned rights. Reference herein to any specific commercial product, process, or service by trade name, trademark, manufacturer, or otherwise, does not necessarily constitute or imply its endorsement, recommendation, or favoring by the United States Government or the University of California. The views and opinions of authors expressed herein do not necessarily state or reflect those of the United States Government or the University of California, and shall not be used for advertising or product endorsement purposes.

Magnetic Field Line Tracing Calculations for Conceptual PFC Design in the National Compact Stellarator Experiment

R. Maingi^a, T. Kaiser^b, D.N. Hill^b, J.F. Lyon^a, D. Monticello^c, M.C. Zarnstorff^c

^a Oak Ridge National Laboratory

^b Lawrence Livermore National Laboratory

^c Princeton Plasma Physics Laboratory

The National Compact Stellarator Experiment (NCSX) is a three-field period compact stellarator presently in the construction phase at Princeton, NJ. The design parameters of the device are major radius $R=1.4\text{m}$, average minor radius $\langle a \rangle = 0.32\text{m}$, $1.2 \leq$ toroidal field (B_t) $\leq 1.7\text{ T}$, and auxiliary input power up to 12 MW with neutral beams and radio-frequency heating. The NCSX average aspect ratio $\langle R/a \rangle$ of 4.4 lies well below present stellarator experiments and designs, enabling the investigation of high β physics in a compact stellarator geometry. Also the NCSX design choice for a quasi-axisymmetric configuration aims toward the achievement of tokamak-like transport. In this paper, we report on the magnetic field line tracing calculations used to evaluate conceptual plasma facing component (PFC) designs.

In contrast to tokamaks, axisymmetric target plates are not required to intercept the majority of the heat flux in stellarators, owing to the nature of the 3-D magnetic field footprint.

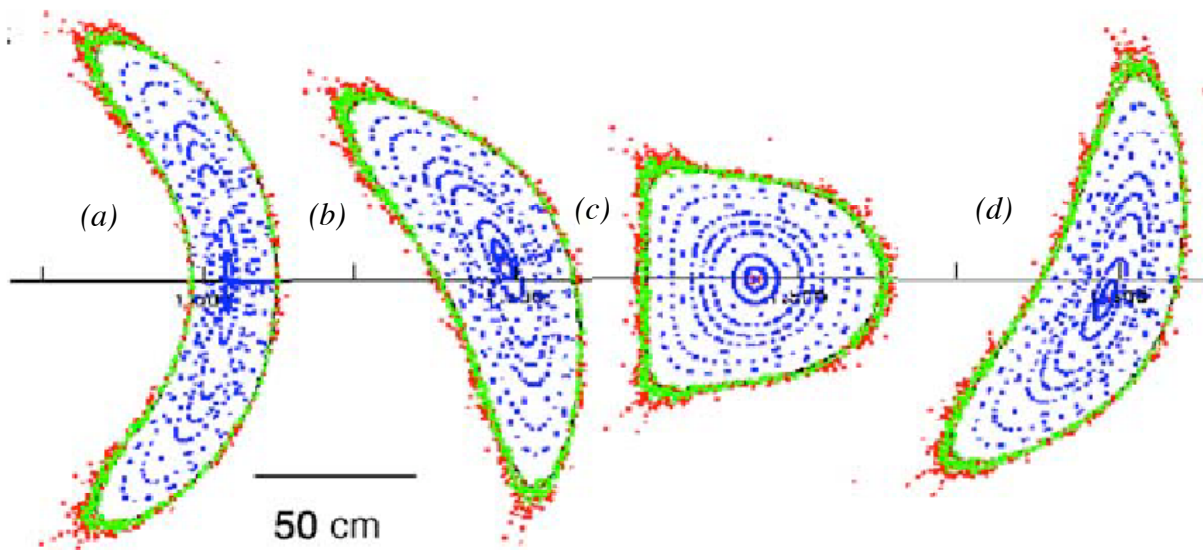


Fig. 1 – Poincaré plots from field lines traced from a full-current, high beta equilibrium¹. The red (green) field lines were launched from the inner (outer) midplane.

The divertor plate design investigated in this study covers approximately one half of the toroidal extent in each period. Typical Poincare plots in Figure 1 illustrate the plasma cross-section at several toroidal angles for a computed NCSX high-beta equilibrium. The plates used for these calculations are centered in each period about the elongated cross-section shown in Figure 1a, extending to $\pm \pi/6$ in each direction.

Two methods for tracing the edge field line topology were used in this study. The first entails use of the VMEC/MFBE-2001 packages^{1,4}, whereas the second entails use of the PIES code⁵ with a post-processor by Michael Drevlak; the same field line integration routine was used to evaluate the equilibria for this comparison⁶. Both inputs were generated based on the $\beta=4\%$, $iota=0.5$ equilibrium computed from the final NCSX coil set. We first compare these two methods for a specific plate geometry, and conclude with a comparison of the strike characteristics for two different target plate poloidal lengths using the latter method.

The details of the magnetic topology differ when computed with VMEC/MFBE as compared with an iterated PIES solution. This difference is illustrated in Figure 2. The presence of islands in the PIES solution effectively reduces the radius of the last closed magnetic surface (LCMS) by about 8 cm. As expected, this difference in the edge topology translates to a difference in field line terminations.

To quantify the impact of the VMEC/MFBE and PIES equilibrium differences on target

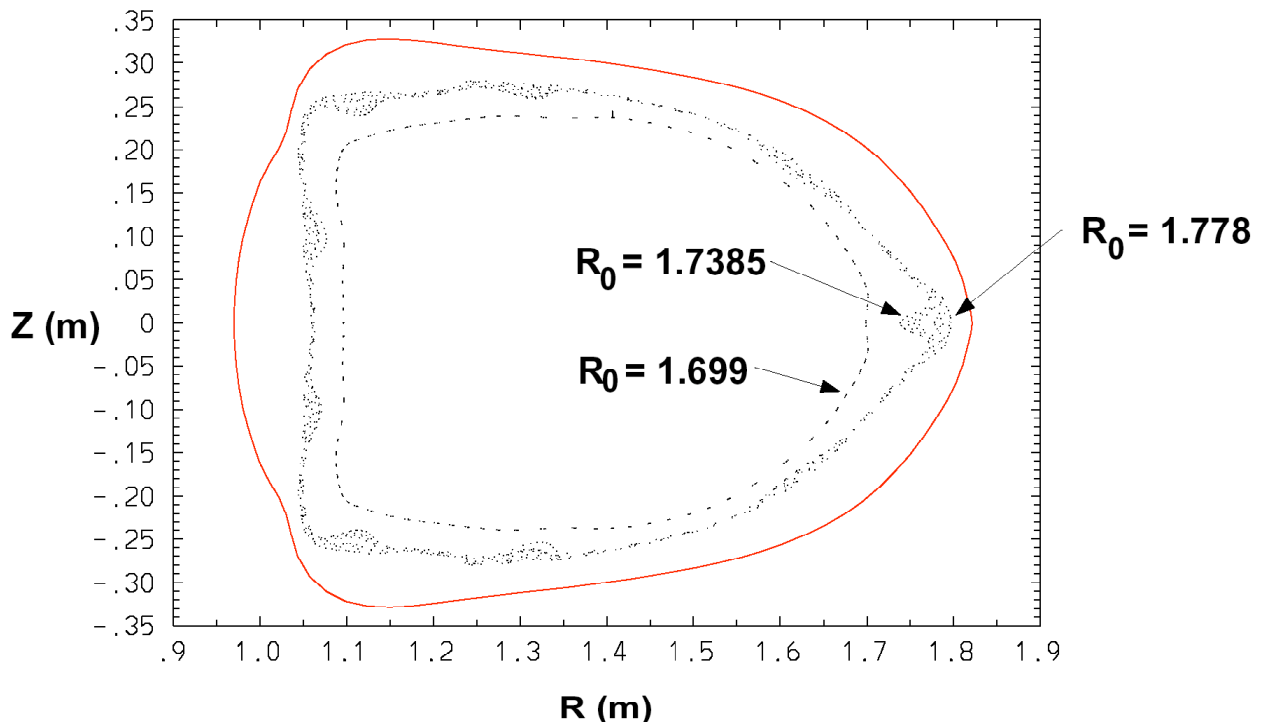


Fig. 2 – Comparison of VMEC and PIES equilibria for code comparison. The last closed magnetic surface from PIES is effectively 8cm inboard of the one from VMEC

footprints, 1000 field lines were launched from the $\phi=0^0$ toroidal angle location in each equilibrium. Target plates of 10 cm poloidal length with a toroidal extent of $\pm \pi/6$ were used. The projections of these plates are shown for several cross-sections in Figure 3. Note that the area behind the target plates separated from the vessel wall is indicated as the divertor shadow region. Particle diffusion was simulated with a field line cross-field diffusion rate of $1 \text{ m}^2/\text{s}$. Field lines were followed until they terminated at the divertor target, in the divertor shadow region, or at the wall. The field line tracing was also terminated if the field line length exceeded 1000 m, because that length would be sufficient to radiate away the parallel heat flux prior to reaching a surface.

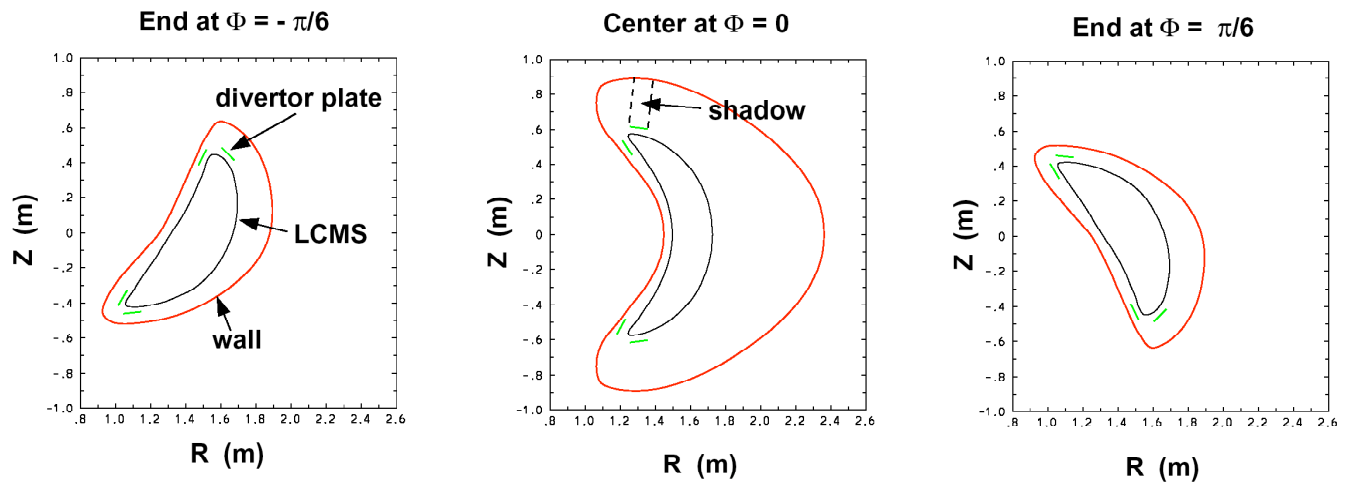


Fig. 3 – Poloidal cross-section at several toroidal angles with location of 10cm long upper and lower divertor plates.

Table 1 shows that the field line termination statistics for the VMEC and PIES equilibria are comparable: most of the field lines terminate at the divertor, and none of the field lines make it to the wall. There are statistically significant minor differences in that more field lines terminate in the divertor shadow region in the PIES equilibrium, but for the equilibrium considered, the field line terminations statistics are similar. Table I also compares the effectiveness of a 10cm long or a 15cm long plate in the PIES equilibrium. The longer plate successfully catches more field lines than the shorter plate, but is not significantly more effective at preventing field lines from entering the shadow region. Additionally, appropriately designed target plates be inserted easily to prevent those field lines in the shadow region from terminating at the wall behind the divertor targets.

In summary, we find that divertor effectiveness is comparable with the VMEC/MFBE equilibrium and the PIES equilibrium for the 10cm long target plate considered. We also find that increasing the poloidal length of the target plate from 10cm to 15cm leads to a marginal improvement in the efficiency as measured by the fraction of field lines impinging on the targets. Detailed sensitivity studies are required for the actual NCSX target plate design, including further variation of the poloidal and toroidal lengths, variation of the plasma/wall gap, variation of the iota profile and the beta in the equilibrium itself. Furthermore a comparison of measured heat and particle flux patterns with predictions from these codes applied to existing or previous stellarators would lend additional credibility for the use of these codes in target design.

We acknowledge discussions with Arthur Grossman (University of California at San Diego). This research was supported by US D.O.E. contracts by the U.S. Dept. of Energy under contracts DE-AC05-00OR22725, W-7405-ENG-48 (UC, LLNL), and DE-AC02-76CH03073.

Table 1 – Comparison of field line terminations with the VMEC/MFBE and PIES equilibria.

| Field line termination | VMEC/MFBE (10 cm) | PIES (10 cm) | PIES (15 cm) |
|------------------------------------|----------------------|-----------------|-----------------|
| Hit any divertor | 84 | 69 | 82 |
| Hit lower outboard divertor | 48 | 29 | 38 |
| Hit upper outboard divertor | 36 | 23 | 23 |
| Hit lower inboard divertor | 0 | 10 | 10 |
| Hit upper inboard divertor | 0 | 7 | 11 |
| Entered Divertor shadow region | 8 | 18 | 17 |
| Length > 1000m (stopped following) | 8 | 13 | 1 |
| Hit vacuum vessel wall | 0 | 0 | 0 |

References

- ¹ P. K. Mioduszewski, *J. Nucl. Materials* **313-316**, 1304 (2003).
- ² S. P. Hirshman, *Comput. Phys. Comm.* **43**, 143 (1986).
- ³ E. Strumberger, *Nuclear Fusion* **37**, 19 (1997).
- ⁴ A. Grossman, *J. Nucl. Materials* **337-339**, 400 (2005).
- ⁵ A. H. Reiman, *Computer Physics Comm.* **43**, 157 (1986).
- ⁶ T. B. Kaiser, *Bull. Am. Phys. Soc.* **49**, 313 (2004).